

**University of Toledo REU Program  
Summer 1998**

**Atomic Force Microscopy Analysis of Microstructure Evolution and Morphology of  
Magnetron-Sputtered CdS Thin Films**

**Ryan Snyder, Kenyon College**

**Advisor: Prof. Jacques G. Amar, University of Toledo**

**ABSTRACT**

Using atomic force microscopy, the surface morphology and microstructure of magnetron-sputtered CdS thin-films grown at 250 C on glass substrates were studied as a function of film-thickness with thicknesses ranging from 50 Å to 1 μ. For each thickness, the height-height difference and product correlation functions  $G(r)$  and  $G_2(r)$  were used to calculate the surface width and typical grain size  $r_c$ . From these results, values for the growth exponent  $\beta = 0.82$ , surface roughness exponent  $\alpha = 0.5 - 0.7$  and coarsening exponent  $n = 0.7$  were calculated. For small and intermediate thicknesses, anomalous scaling of the height-difference correlation function was observed, indicating an increase of the average grain angle with thickness as well as a large distribution of grain-angles. However, at large thicknesses the average grain angle was found to saturate while the grain angle distribution narrowed. The large value of  $\beta$  as well as the rapid increase in the average grain angle at small and intermediate thicknesses indicate the existence of an instability during the sputter deposition process. We conjecture that this instability is due to “shadowing” which occurs as a result of scattering of incoming Cd and S atoms by the Ar plasma during the deposition process and leads to a range of incident angles for deposition. Such instability can lead to grooves between the grains and “pinholes” which can destroy a completed CdS/CdTe solar cell. We suggest some methods to eliminate shadowing during the deposition process and thus eliminate the instability.

## I. Introduction

In this work, we studied the kinetics of growth for CdS on boron-magnetron sputtering at  $250^\circ\text{C}$ . CdS is a n-type material used in creating the junction in a solar cell. It was our objective in this study to learn more about the mechanism of these films from magnetron sputter deposition. We hope to develop ideas on how to grow a more efficient solar cell. These results are used to guide future computer simulations of the thin-film deposition.

Atomic force microscopy (AFM) was used to collect height information on CdS films, and the data collected allowed us to study the morphology of CdS at various thicknesses. AFM was developed from the Scanning Tunneling Microscope; it uses a small cantilever (about 0.1 mm long) with a small tip. The cantilever is positioned underneath the sample, and the cantilever is scanned line by line across the sample with the tip in direct contact with the sample surface. A laser beam from a scanner head of the AFM is directed at a mirror that must be adjusted so that the beam directly over the tip. The forces between the tip and the cantilever cause the cantilever to bend, and a position-sensitive photodetector (PSPD) measures the deflection of the laser beam as the sample is moved under the tip. This converts the displacements of light as small as 10 angstroms. The ratio of the photodetector and the cantilever to the length of the cantilever itself results in a large amplification. This allows sub-angstrom resolution in the vertical direction. The capability of the AFM to carry out small scan sizes allows for a complete scan in the horizontal direction.

As the tip of the AFM is brought closer to the surface, the attractive van der Waals forces. This attraction increases until the atoms of the tip and sample are brought so close together that their electron clouds begin to repel each other electrostatically. This repulsion weakens the van der Waals force as the tip and sample separation continues to decrease. The total force goes to zero when the tip and sample reach a couple of angstroms apart, about the length of a chemical bond. If the tip force becomes positive (repulsive), the tip and sample are in contact. The electrostatic force balances any force that tries to push the tip away from the sample. When the cantilever pushes the tip against the sample, the cantilever is bent, forcing the tip and sample atoms closer together. Due to this electrostatic repulsion, care must be taken to ensure that the tip does remain in contact with the sample. The repulsive force can occasionally force the tip away from the sample, resulting in a loss of resolution.

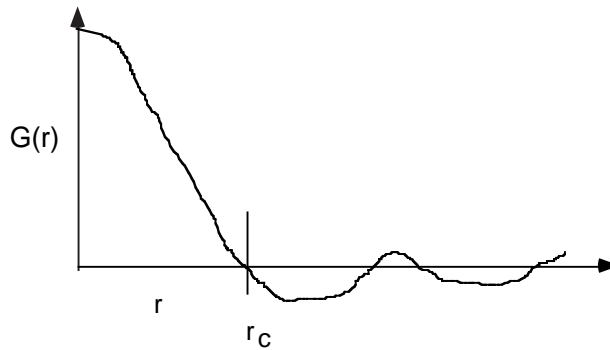
## II. Analysis

The surface morphology of the CdS thin films was quantitatively analyzed using the height-difference correlation function. The height-height correlation function is  $G(r)$  where  $r$  is the distance from a selected origin in the plane of the film.  $G(r) = \langle [h(r) - h(0)]^2 \rangle$  where  $h(r)$  is the height of the film a distance  $r$  from the origin in the plane of the film and  $h(0)$  is the height of the film at the origin. The value for the difference is

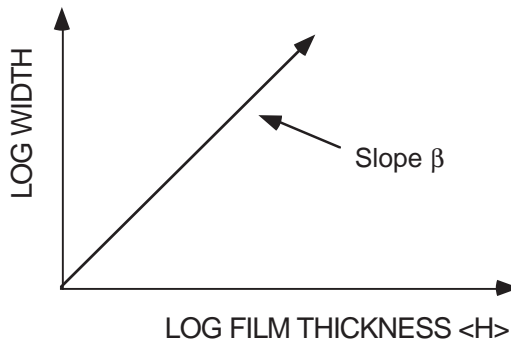
averaged over the entire surface. The height-height correlation function is represented by the expression  $\langle (h(0) - \langle h \rangle)(h(r) - \langle h \rangle) \rangle$  where  $\langle h \rangle$  is the average height of the sample.

At small length scales, one expects  $G_2(r) \propto r^{-2\alpha}$  where  $\alpha$  is the roughness exponent. However, at larger length scales the value at which  $G_2(r)$  saturates would be expected to increase with thickness since the height difference at larger length scales. The distance  $r$  from the origin at which saturation occurs should increase with thickness as well since the grains coarsen as the film thickness increases. Normally, the value of  $G_2(r)$  at small distances from the origin would not be expected to change with increasing thickness. However, if the value of  $G_2(r)$  at small  $r$  increases with film thickness, this indicates that the grains are coarsening with increasing thickness.

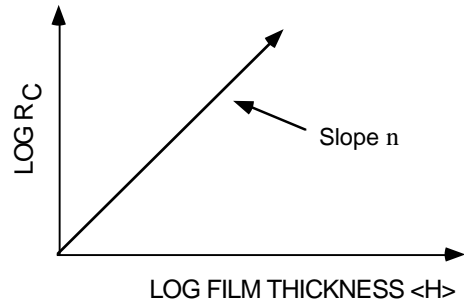
The  $G(r)$  graph shown below shows that the  $G(r)$  curve crosses the zero value at  $r_c$  which is approximately the lateral size of the grains.



The square root of  $G(r)$  at  $r = 0$  is the root mean square (rms) fluctuation, sometimes known as the width. The width is expected to vary as  $\langle h \rangle^\beta$  where  $\beta$  is the growth exponent.



The  $\beta$  value varies with  $n$  where  $n$  is the coarsening exponent, and its value indicates how fast the lateral size of the grains are growing with increasing thickness. The rms width (see Fig. 4) was also plotted as a function of film thickness to provide information about the angle at which the grains of CdS were growing.



A computer program was written to calculate  $G(r)$  from the AFM height function of distance from an origin. For each sample width, values for  $r$  and  $\alpha$  were calculated and the width values for each sample were used to measure  $\beta$ , respectively.

### Results

Figure 1 shows the correlation function  $G(r)$  for a typical sample thickness for this plot was 2000 Angstroms, and the curve crosses the x-axis is approximately 500 angstroms.

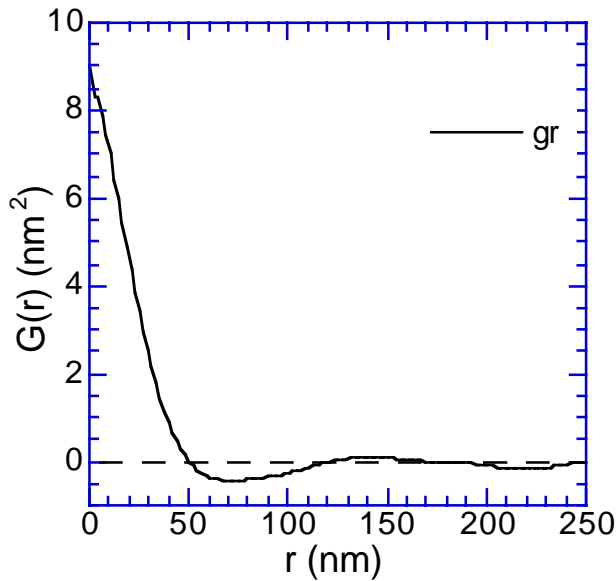


Figure 1.  $G(r)$  curve for a 2000 A sample of CdS on BSG

Figure 2 shows the  $G_2(r)$  curves for all samples grown on BSG glass. It is seen (except for the 5000 Å sample) that as each sample begins to saturate, the initial value of  $G_2(r)$  increases with sample thickness. The point where each curve begins to saturate is expected since the surface should become rougher due to more variability in grain size. At initial  $r$  values for the thinner samples (50 – 300 Å) the slope of the grains is increasing. The samples from 500-2000 Å all start with initial values for  $G_2(r)$  around 0.6 indicating that the angles at which grains are choosing to grow is still very random. The samples with thicknesses of 10000 Å and 100000 Å give values of 0.7 (close to 1) indicating the grains are starting to grow at a preferred angle at which to grow.

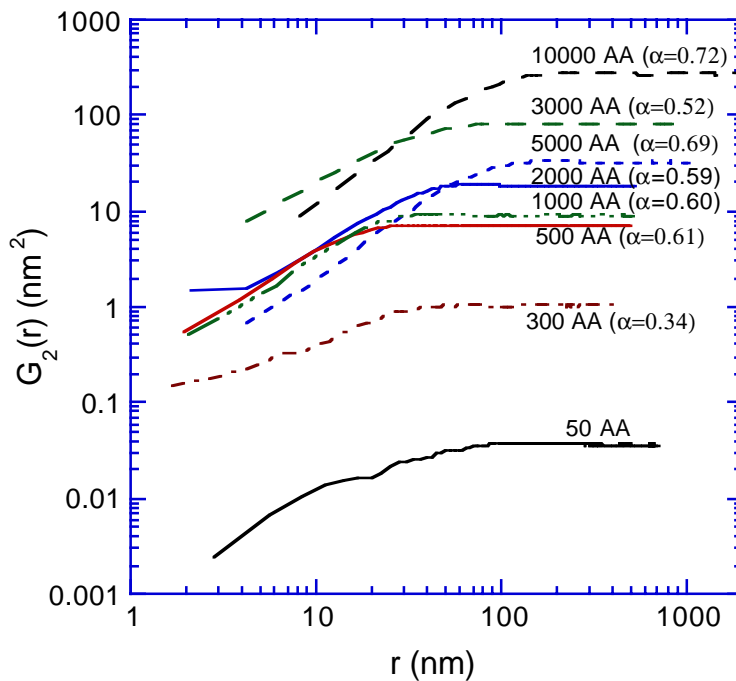


Figure 2. The  $G_2(r)$  curves for sample thicknesses from 50 to 10000 Å

Figure 3 displays the width as a function of film thickness. The growth exponent  $\beta$  indicates a value for the growth exponent. This indicates a possible instability because the rms width is growing almost as fast as the thickness. Figure 3 does show that the samples are becoming rougher for increasing thickness: the roughness is growing much faster than expected.

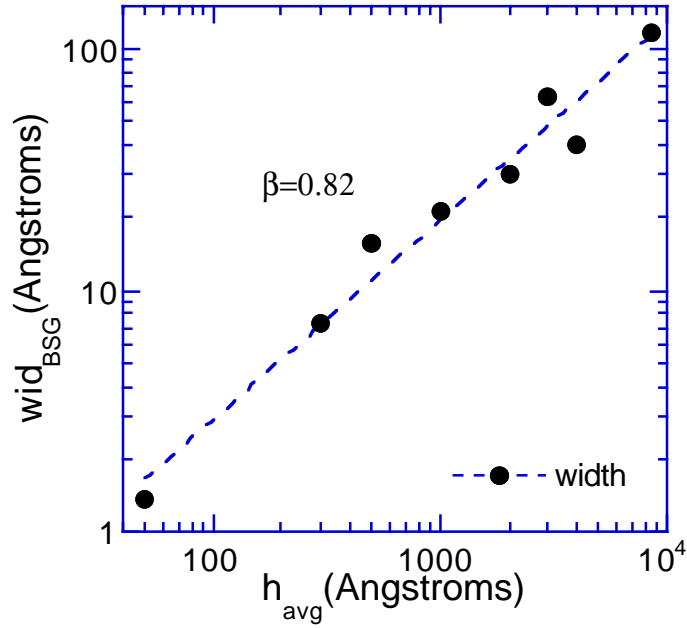


Figure 3. The root-mean square width of  $G(r)$  with  $r = 0$  for sample thicknesses

Figure 4 shows how the  $r_c$  values as a function of film thickness. The coarsening exponent calculated with a fit to the last 6 data points was 0.69. The first two data points on Figure 4, corresponding to f:

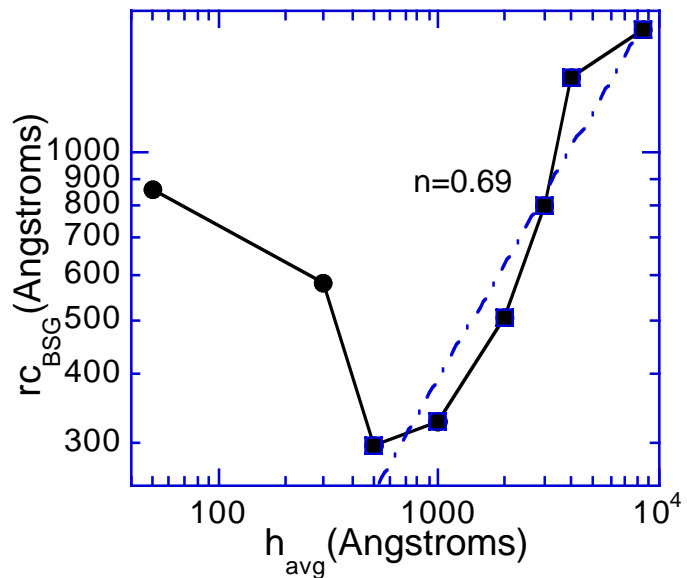


Figure 4.  $r_c$  as a function of sample thickness with a power law fit to the data to measure the coarsening exponent  $n$



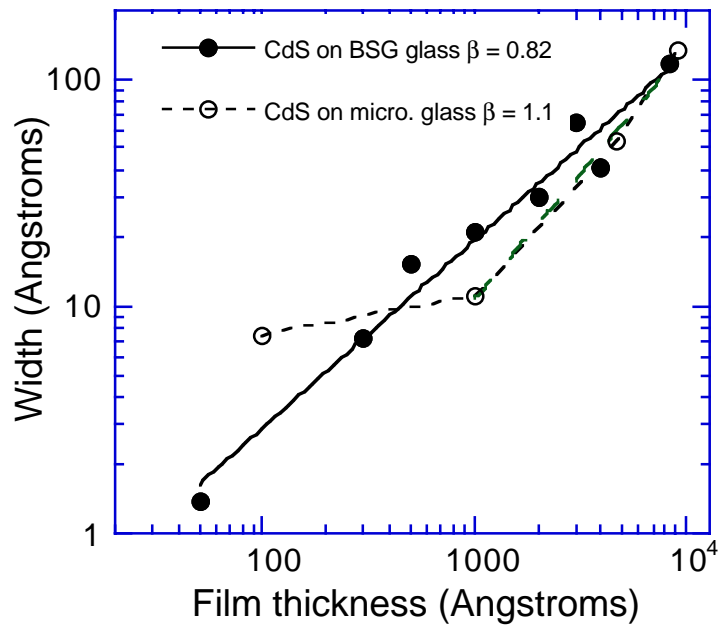


Figure 6. Comparison of rms width as a function of film thickness for CdS deposited on BSG glass and microscope glass

## Conclusions

There have been great efforts devoted to understanding the kinetic roughening of growing surfaces with various techniques. Jeffries, Zuo, and Craig [1] studied the growth of Pt sputter deposited on glass at room temperature for film thicknesses of 15-140 nm. A roughness exponent ( $\alpha = 0.9$ ) and a growth exponent ( $\beta = 0.3$ ) were measured to conclude that the growth was consistent with linear diffusion dynamic. Krim [2] studied scaling behaviors of vapor-deposited silver onto quartz at room temperature and found similar results for the roughness exponent ( $\alpha = 0.9$ ) and growth exponents ( $\beta = 0.29$ ). Zeng and Vidal [3] measured similar values for growth (roughness exponent = 0.9) for growth of Pb on Cu(100) using helium beam at 150 K.

Our results differ from those presented above. Our roughness exponent is smaller, and it indicated that our samples needed to be grown higher to saturate and approach a preferred angle of growth. The lower value of roughness exponent in our experiments may be due to the higher growth temperature of 250 C used in our experiments. It should be mentioned that the magnetron-sputtering process for these samples involved Ar ions hitting a target and knocking off the CdS. The ejected CdS then travels through an Ar plasma before being deposited on the substrate. Collisions with the Ar plasma most likely lead to a wide range of deposition angles, which may lead to a better understanding of how the Ar plasma interacts with the CdS could help in understanding our results.

The  $r$  values displayed in Figure 4 are very high for the thin samples (below 300 A). A possible explanation for this fact is the initial roughness of the substrate presents data that shows the rms width of CdS deposited on microscope

surface, growing similarly to CdS on BSG. A more complete study of the surface and measurement of the roughness could provide insight into why the roughness values were found for thin samples.

Probably the most interesting result of this work is the growth exponent value of 0.82. The experiments mentioned above attained growth exponent values of 0.3. The possible cause for the large value in our experiment is an effect called shadowing. When CdS is knocked off the target by Ar ions, they travel through the Ar plasma and are deposited on the surface. This Ar plasma interacts with the CdS in such a way that it allows the CdS to be deposited on the surface at a wide range of angles. The CdS toward the surface at these wide angles may be blocked by peaks on the surface previously deposited. This allows the peaks to grow higher and the roughness to increase as fast as a result. CdS will still be deposited in the valleys if it is deposited at a suitable angle, but the large growth exponent indicates that shadowing is taking place.

This rough surface may affect the efficiency of the solar cell. The presence of pinholes inhibiting the function of the pn junction in a CdS/CdTe solar cell. One way to correct for this shadowing effect is to rotate the substrate during the deposition. Changing the conditions of the Ar plasma such as voltage, gas flow, and field strength, etc. may also correct this effect.

These experimental results certainly provide many exciting areas to be studied. Computer simulations can be done to try and model the plasma to come to a better understanding of how it interacts with the CdS. More AFM work can be done with microscope glass as the substrate and with SnO<sub>2</sub> coated glass which is currently the substrate used for CdS/CdTe solar cells.

## References

- [1] J.H. Jeffries, J.-K. Zuo, and M.M. Perlman, *Phys. Rev. Lett.* **75**, 4935 (1996).
- [2] G. Palasantzas and J. Kanich, *JPhys. Rev. Lett.* **73**, 3564 (1994).
- [3] H. Zeng and G. Vidale, *Phys. Rev. Lett.* **74**, 582 (1995).